Internet Electronic Journal of Molecular Design **2004**, *3*, 163–181 ISSN 1538–6414
BioChem Press http://www.biochempress.com

Inter*net* Electronic Journal of Molecular Design

April 2004, Volume 3, Number 4, Pages 163–181

Editor: Ovidiu Ivanciuc

Special issue dedicated to Professor Nenad Trinajstić on the occasion of the 65th birthday
Part 10

Guest Editor: Douglas J. Klein

Tautomerism and Non–planarity of the Amino Group in 4(7)–Aminobenzimidazole: A Theoretical and Matrix–isolation FT–IR Study

Linda Houben,[1] Riet Ramaekers,[1] Ludwik Adamowicz,[2] and Guido Maes[1]

[1] Department of Chemistry, University of Leuven, Celestijnenlaan 200F, B–3001 Leuven, Belgium
[2] Department of Chemistry, University of Arizona, Tucson, USA

Received: November 28, 2003; Revised: February 12, 2004; Accepted: February 17, 2004; Published: April 30, 2004

Citation of the article:
L. Houben, R. Ramaekers, L. Adamowicz, and G. Maes, Tautomerism and Non–planarity of the Amino Group in 4(7)–Aminobenzimidazole: A Theoretical and Matrix–isolation FT–IR Study, *Internet Electron. J. Mol. Des.* **2004**, *3*, 163–181, http://www.biochempress.com.

Inter*net* Electronic Journal of Molecular Design

BioChem Press
http://www.biochempress.com

Tautomerism and Non–planarity of the Amino Group in 4(7)–Aminobenzimidazole: A Theoretical and Matrix–isolation FT–IR Study[#]

Linda Houben,[1] Riet Ramaekers,[1] Ludwik Adamowicz,[2] and Guido Maes[1,*]

[1] Department of Chemistry, University of Leuven, Celestijnenlaan 200F, B–3001 Leuven, Belgium
[2] Department of Chemistry, University of Arizona, Tucson, USA

Received: November 28, 2003; Revised: February 12, 2004; Accepted: February 17, 2004; Published: April 30, 2004

Internet Electron. J. Mol. Des. **2004**, *3* (4), 163–181

Abstract

The tautomeric equilibrium 4–NH_2–benzimidazole ⇆ 7–NH_2–benzimidazole has been investigated using a combined theoretical (DFT (B3LYP)/6–31++G**) and experimental (matrix–isolation FT–IR) methodology. The 4–NH_2 tautomer appears to be the most abundant form in a low temperature Ar matrix in accordance with the theoretical predictions. The rare 7–NH_2 form is sufficiently abundant to be vibrationally characterized in detail. The obtained results have allowed to analyze the non–planarity of the NH_2 group, which is particularly large in the 7–NH_2 tautomer. This appears to be at the origin of a large deviation between predicted and experimental frequencies of the NH_2 wag mode. The latter effect has also been observed for other compounds with a NH_2 group in close proximity of an N–H group.

Keywords. Matrix–isolation; FT–IR spectroscopy; theoretical calculations; tautomerism, anharmonicity; non–planar NH_2 group.

1 INTRODUCTION

Since a number of years, we have been studying the tautomerism and H–bonding characteristics of the different DNA and RNA bases uracil, thymine, cytosine, adenine and guanine [1–10]. One of the most suitable investigation methods is the combination of moderate to high level *ab initio* calculations with matrix–isolation Fourier–transform infrared spectroscopy. The theoretical methods of sufficient level allow to predict geometries, energies and vibrational frequencies with good accuracy. Application of the faster DFT methodology has opened new possibilities for larger molecules. On the other hand, the sharpness of the IR absorption of samples isolated in low temperature inert matrices allows observation of separated, close lying bands of different tautomers and/or complexes more easily than in solution or in the solid state. Furthermore, combination of the two methods offers two additional advantages, *i.e*. a good control of the reliability of the theoretical

[#] Dedicated to Professor Nenad Trinajstić on the occasion of the 65th birthday.

* Correspondence author; phone: 0032–167450; fax: 0032–16327992; E–mail: Guido.Maes@chem.kuleuven.ac.be.

methodologies and an ideal simulation of intrinsic tautomeric and/or H–bonding parameters, free of perturbation by an interacting environment.

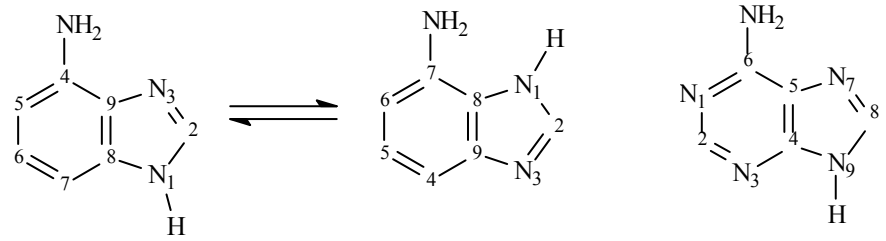

Figure 1. Schematic representation of 4(7)–NH_2–benzimidazole (left) in comparison with adenine (right).

Before the study of the DNA base adenine [11], we have performed an investigation of suitable, simpler model compounds. The compound 4(7)–NH_2–benzimidazole was one of those compounds modeling for one of the (several) tautomerizations of the DNA base adenine [11], since it also presents the interesting tautomerism between the N_9H and the N_7H group. While there are no N atoms present in the six ring part, which prevents both the six ring amino ⇆ imino and N_iH ⇆ N_jH tautomerisms occurring in adenine, the NiH ⇆ NjH prototropy in the five ring (imidazole) part may occur. It should be mentioned that the IUPAC numbering of the six ring and five ring atoms is totally different between 4(7)–NH_2–benzimidazole and adenine (see Figure 1). The numbering in benzimidazoles starts at the NH group towards the N atom in the imidazole ring. This results in a different number for the C atom carrying the NH_2 group, although the latter keeps the same position on the six ring. This gives rise to the recommended names 4–NH_2–benzimidazole and 7–NH_2–benzimidazole.

No data on the tautomerization and IR spectra of 4(7)–NH_2–benzimidazole are available in the literature, which is limited to other aspects such as the synthesis [12] and the reactivity [13,14] of the compounds. This is rather surprising since the problem of the non–planarity between the NH_2 group and the adjacent heterocyclic six ring in adenine is well known [15]. Vibrational spectroscopy is a very suitable method to investigate this non–planarity, since this should effect the out–of–plane NH_2–modes, *e.g.* the wag NH_2 mode. This aspect has been an additional motivation for the present study.

2 MATERIALS AND METHODS

2.1 Theoretical Method

The geometry and energies of the two 4(7)–NH_2–benzimidazole tautomers have been calculated with the density functional theory (DFT) method. We have used the hybrid of Becke's non–local three parameter exchange and correlated functional with the Lee–Yang–Parr correlation functional (B3LYP) [16,17]. In these calculations, the standard 6–31++G** basis set was employed. The IR frequencies and intensities have also been computed at the DFT level of theory using the harmonic

approximation and the analytical derivative procedure incorporated in the GAUSSIAN 94 program [18]. Finally, the potential energy distribution (PED) analysis has been performed and the harmonic DFT IR frequencies have been scaled down to approximately account for the various systematic errors in the theoretical approach. A set of different scaling factors was used, reflecting the difference in anharmonicity of the different types of vibrational modes, *i.e*. 0.950 for ν(XH), 0.980 for out–of–plane modes and 0.975 for all other modes. The use of different scaling factors for frequencies belonging to different types of vibrational modes has been proposed by several authors [19–21]. In some cases, also the restricted Hartree–Fock (RHF) and Möller–Plesset (second order) perturbation (MP2) calculation methods with the same basis set (6–31++G**) have been used for sake of comparison. The calculation of the potential energy variation in the wag mode of the NH_2 group has also been performed using DFT (B3LYP)/6–31++G**. For this purpose, the two dihedral angles C–C–N–H for the H atoms of the amino group attached to the six ring part were constantly varied by 10° (or 5° near the minimum) while optimizing the remaining geometry parameters of 4(7)–NH_2–benzimidazole.

2.2 Experimental Method

The high–purity argon gas (N60 = 99.9999%) was obtained from Air Liquide. The compound 4(7)–NH_2–benzimidazole was synthesized according to the procedure described by Fisher *et al*. [12]. The final product was obtained in high purity quality as checked by ^{1}H and ^{13}C NMR spectroscopy after chromatography on silica with CH_2Cl_2/CH_3OH as eluent followed by vacuum sublimation.

The cryogenic equipments used for the matrix isolation experiments have been described in detail in earlier papers [1,22]. The solid compound was evaporated using a home–made mini furnace, installed in the cryostat. The optimal sublimation temperature for the monomeric compound was found to be 340 K. At this temperature, all bands due to H–bonded dimers have completely disappeared after comparison with dimer spectra [11]. The IR spectra (4000–400 cm^{-1}) of the matrix–isolated samples were obtained by Fourier transforming 64 interferograms on a Bruker IFS–88 instrument at a resolution of 1 cm^{-1}, with a pyroelectric DTGS detector and a KBr beamsplitter. In order to check the thermal stability of the compound during the experiment, IR spectra of KBr pellets of the compound before and after heating in the furnace were compared.

3 RESULTS AND DISCUSSION

3.1 Geometries and Energies

We have first calculated the relative energies of the two tautomers 4–NH_2–benzimidazole and 7–NH_2–benzimidazole. Figure 2 depicts the geometries of both tautomers optimized at the DFT (B3–LYP)/6–31++G** level of theory. It is clearly observed from Figure 2 that the orientation of the NH_2 group is different in the two tautomers, this group being deviated from the benzimidazole

six ring molecular plane: the DFT calculated Z–coordinates for the H atoms of the NH_2 group are 0.1584 and 0.2904 for the 4–NH_2 form and 0.6517 and –0.0179 for the 7–NH_2 tautomer. It is obvious that the exocyclic amino group can be positioned at either side of the aromatic plane, giving rise to two stable conformational structures for each tautomer. Both mirror conformations of each tautomer are of course energetically and vibrationally completely identical.

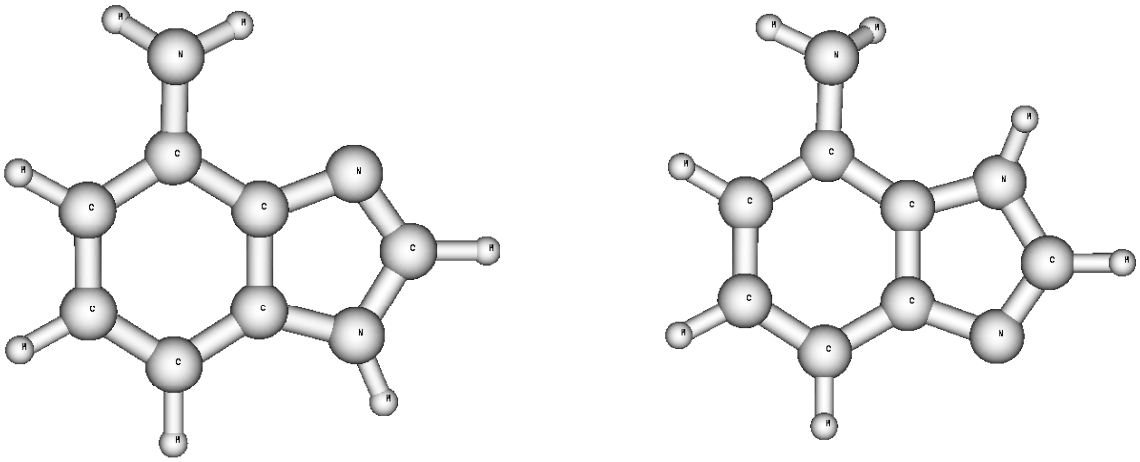

Figure 2. DFT(B3LYP)/6–31++G** optimized geometry of 4–NH_2–benzimidazole (left) and 7–NH_2–benzimidazole (right).

Table 1. *Ab initio* and DFT (B3LYP) calculated energy components, relative energies E_{rel} and dipole moments μ for 4–NH_2–benzimidazole and 7–NH_2–benzimidazole (6–31++G** basis set)

Method	4–NH_2–Benzimidazole	7–NH_2–Benzimidazole
DFT (a.u.)	–435.259577	–435.253330
MP2 [a] (a.u.)	–433.963791	–433.958867
RHF (a.u.)	–432.539949	–432.534534
ZPE (DFT) [b] (a.u.)	0.130948	0.130858
ZPE (RHF) [c] (a.u.)	0.130491	0.130454
E_{rel} (DFT) (kJ.mol^{-1})	0.00	16.07
E_{rel} (MP2) (kJ.mol^{-1})	0.00	12.83
E_{rel} (RHF) (kJ.mol^{-1})	0.00	14.12
μ (DFT) (D)	2.22	4.39
μ (RHF) (D)	2.68	4.15

[a] Only valence correlation is considered
[b] Calculated as $0.97\Sigma h\nu_i/2$ with ν_i, the frequencies at the DFT level
[c] Calculated as $0.90\Sigma h\nu_i/2$ with ν_i the frequencies at the RHF level

The theoretical energy results are summarized in Table 1. It appears that, at the DFT (B3LYP)/6–31++G** level of theory, the 4–NH_2 tautomer is the most stable form, the relative energy compared to the 7–NH_2 form being about 16 kJ mol^{-1}. For sake of comparison, we have also calculated the relative energies at the RHF and MP2 levels of theory using the same basis set. The relative energies are about 14 and 13 kJ mol^{-1}, respectively. These energy values suggest that the less stable 7–NH_2 tautomer should be observed in minor amounts in low–temperature Ar matrices. As a matter of fact, former studies, *e.g.* on 2–pyridone ⇆ 2–hydroxypyridine in Ar, have demonstrated that both tautomers can be easily identified in Ar when the energy difference is not larger than about 15 kJ mol^{-1} [23].

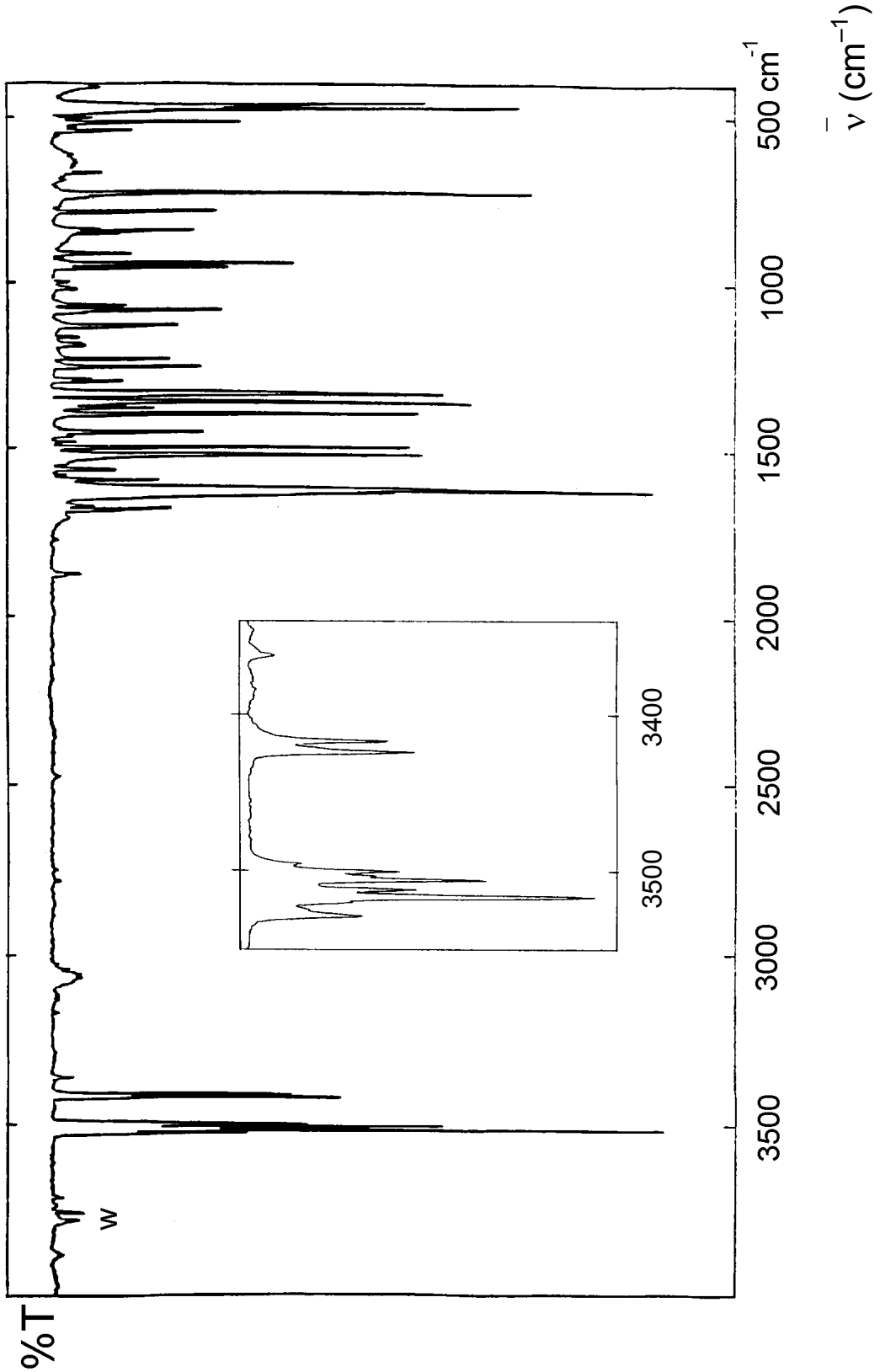

Figure 3. FT–IR spectrum of 4(7)–NH_2–benzimidazole in Ar at 10 K (furnace temperature 340 K ; w = water impurity).

3.2 Vibrational Analysis

4(7)–NH_2–Benzimidazole (N = 17) has 45 vibrational modes which, under C_s symmetry of the rings plane of the ring system, can be divided into 27 in–plane (A') and 12 out–of–plane (A'') ring modes and 4 in plane (A') and 2 out–of–plane (A") NH_2 modes. Figure 3 illustrates the monomer IR spectrum of 4(7)–NH_2–benzimidazole isolated in Ar at 10 K. Apart from the very weak bands in the spectral regions 3800–3700 cm^{-1} and 3300 cm^{-1} due to a very small amount of water impurities (free 3800 cm^{-1}; complex 3290 cm^{-1}), no other bands due to contaminants or self–association of the compound in the matrix sample are observed. Comparison of the spectra with spectra for 4(7)–NH_2–benzimidazole·H_2O complexes obtained from a separate study [11] allows to exclude the presence of any H–bonded complex with those water impurities. Inspection of Figure 3 immediately indicates the presence of both tautomers 4–NH_2– and 7–NH_2–benzimidazole, since the number of intense to medium intense bands observed in the experimental spectrum is larger than expected for only one tautomer. This is illustrated by the frequency region 3550–3300 cm^{-1} where only three modes $\nu^a(NH_2)$, $\nu^s(NH_2)$ and $\nu(N_1H)$ are expected for a single tautomer. As a matter of fact, 7 intense bands are observed in that spectral region.

Table 2. Experimental (Ar matrix) and calculated (RHF and DFT–B3–LYP/6–31++G**) vibrational data for 4–NH_2–benzimidazole

Experimental ν (cm^{-1})	Calculated ν (cm^{-1})			Experimental [a] I (km mol^{-1})		Calculated A (km mol^{-1})		PED [e]		
	RHF [b]	DFT [c]	DFT [d]	RHF	DFT	RHF	DFT	Mode	RHF	DFT
3517/3512 [f]	3533	3585	3512	53	21	37	28	$\nu^a(NH_2)$	100	100
3506/3500	3534	3563	3489	84	105	103	67	$\nu(N_1H)$	99	100
3423/(3416?)	3428	3471	3400	50	36	39	32	$\nu^s(NH_2)$	100	99
3079	3078	3158	3093			4	1	$\nu(C_2H)$	99	99
3055	3035	3111	3047			16	14	$\nu(C_7H)$ $\nu(C_6H)$	64 34	76 21
3041	3018	3094	3031	51[g]	36[g]	19	16	$\nu(C_6H)$ $\nu(C_5H)$ $\nu(C_7H)$	34 39 26	51 27 22
3028	3003	3079	3015			11	11	$\nu(C_5H)$ $\nu(C_6H)$	62 34	71 27
1623	1630	1613	1621			227	231	$\delta(NH_2)$	58	45
1631	1627	1610	1618	338[g]	241[g]	50	34	$\nu(C_7C_8)$ $\nu(C_4C_9)$	16 14	20 17
1587	1598	1583	1591	9	6	20	8	$\delta(NH_2)$ $\nu(C_8C_9)$	27 17	40 11
1516	1507	1504	1512	39	28	39	64	$\delta(C_5H)$ $\nu(C_4C_5)$	20 13	17 16
1493	1538	1491	1498	108	77	108	77	$\nu(C_2N_3)$ $\delta(C_4N)$ $\nu(C_2H)$	59 – 17	58 20 –
1446	1444	1431	1439	16	11	15	21	$\delta(C_7H)$ $\nu(C_8C_9)$	27 18	26 18
1393	1229	1387	1395	9	6	14	21	$\delta(N_1H)$ $\delta(C_6H)$ $\nu(C_7C_8)$	11 17 15	17 13 –

Table 2. (Continued)

Experimental ν (cm^{-1})	Calculated ν (cm^{-1})			Experimental [a] I (km mol^{-1})		Calculated A (km mol^{-1})		PED [e]		
	RHF [b]	DFT [c]	DFT [d]	RHF	DFT	RHF	DFT	Mode	RHF	DFT
1333	1398	1350	1357	94[g]	67[g]	84	42	$\delta(N_1H)$	39	20
								$\nu(C_8C_9)$	–	18
								$\nu(N_1C_2)$	15	14
1335	1295	1320	1326			87	61	$\nu(C_4N)$	28	22
1253	1259	1287	1293	15	19	8	14	$\delta(C_5H)$	28	26
								$\nu(N_3C_9)$	–	15
								$\delta(C_7H)$	20	–
1229	1217	1236	1243	10	7	9	12	$\nu(N_3C_9)$	23	23
1189/1186	1335	1216	1222	9	6	9	6	$\delta(C_2H)$	33	25
								$\nu(C_2N_3)$	15	12
1131	1136	1152	1158			0.5	3	$\delta(C_6H)$	–	24
								$\delta(C_7H)$	16	23
								$\nu(C_6C_7)$	15	–
1128	1104	1115	1120	29[g]	21[g]	29	16	$\rho(NH_2)$	–	32
								$\delta(C_5H)$	15	17
								$\nu(C_5C_6)$	17	–
1080	1068	1070	1075	35	25	44	18	$\nu(N_1C_2)$	63	59
								$\delta(N_1H)$	21	25
1065	1047	1054	1059	8	6	9	16	$\nu(C_6C_7)$	20	24
								$\nu(C_5C_6)$	17	13
1015	997	999	1004	7	5	7	6	$\rho(NH_2)$	23	29
								$\nu(C_5C_6)$	17	17
								$\nu(C_4C_5)$	–	15
994	977	923	932	1	1	1	0.6	$\gamma(C_6H)$	83	82
								$\gamma(C_7H)$	15	18
913 or 908	916	913	917	10[g]	7[g]	6	8	δ(r1)	36	40
								δ(r2)	35	35
911	829	835	839			5	5	δ(R1)	43	46
852	851	817	825	4	3	5	10	$\gamma(C_5H)$	34	51
								$\gamma(C_7H)$	66	26
								$\gamma(C_2H)$	–	21
834	906	814	822	7	5	7	5	$\gamma(C_2H)$	100	81
786	775	755	763	20	14	47	15	τ(r2)	19	29
								τ(R1)	24	27
								$\gamma(C_4N)$	17	16
								$\gamma(C_7H)$	20	15
730	735	715	722	81	58	72	70	$\gamma(C_7H)$	29	39
								$\gamma(C_6H)$	18	23
								τ(R1)	21	12
668	665	675	678	3	9	3	0.5	$\nu(C_7C_8)$	21	19
648	641	635	641	0.3	0.1	4	0.7	τ(r1)	61	63
								τ(r2)	–	22
541/539	619	600	607	26	19	57	18	$\gamma(C_4N)$	28	36
								τ(r2)	31	22
605	592	595	598	1	0.7	2	2	δ(r2)	29	29
								$\nu(C_4C_9)$	2	20
								δ(R3)	18	17
514	526	534	540	17	12	24	14	τ(R1)	–	36
								τ(R3)	–	26
								τ(R2)	41	–

Table 2. (Continued)

Experimental ν (cm^{-1})	Calculated ν (cm^{-1})			Experimental [a] I (km mol^{-1})		Calculated A (km mol^{-1})		PED [e]		
	RHF [b]	DFT [c]	DFT [d]	RHF	DFT	RHF	DFT	Mode	RHF	DFT
470	551	512	518	101	72	143	145	wag(NH_2)	38	37
								τ(R2)	–	25
								τ(R1)	22	–
								τ(R3)	21	–
460	494	489	494	83	59	121	133	wag(NH_2)	24	30
								τ(R2)	19	26
								γ(C_6H)	15	–
466	466	467	469	4	3	4	2	δ(R3)	20	22
								δ(R2)	24	21
								δ(C_4N)	17	18
[h]	425	439	444			103	73	γ(N_1H)	99	96
[h]	317	356	360			31	49	τ(NH_2)	87	86
	276	273	276			10	6	τ(R3)	43	45
								τ(R2)	20	19
								τ(r1)	15	15
[h]	264	261	262			9	8	δ(C_4N)	48	51
								δ(R3)	18	19
[h]	214	214	216			27	22	τ(Rr)	70	69
[h]	182	179	181			8	6	τ(R2)	54	57
								τ(R1)	16	16

[a] Experimental intensity normalized to the calculated value of ν(C_2N_3) at 1538 cm^{-1} (108 km.mol^{-1}) for RHF or 1491/1498 cm^{-1} (77 km.mol^{-1}) for DFT
[b] Uniform scaling factor 0.900
[c] Uniform scaling factor 0.970
[d] Variable scaling factor used, i.e. 0.950 for ν(X–H) modes, 0.980 for τ, γ and wag modes and 0.975 for all other modes
[e] Only contributions ≥ 15% are listed; ν designates stretching vibration, σ bending, τ torsion, wag wagging mode, γ out–of–plane vibration, and ρ rocking mode; NH_2 modes are further indicated with 's' for symmetric and 'a' for asymmetric; R and r refer to the six and five ring part, respectively
[f] Most intense band underlined
[g] Separate intensities not measurable
[h] Situated below the studied spectral region (< 400 cm^{-1})

Table 2 summarizes the spectral analysis for the most stable form 4–NH_2–benzimidazole. The vibrational analysis for this tautomer is complete except for the location of the γ(N_1H) which is predicted to be an intense band around 440 to 420 cm^{-1}. Due to its large anharmonicity, this type of out–of–plane mode is usually detected some 5–10% lower, which suggests that this band is situated below 400 cm^{-1}. In view of the analysis of the non–planarity of the NH_2 group (see further), particular attention should be given to the assignment of the out–of–plane NH_2 modes. Apart from the τ(NH_2) modes located below 400 cm^{-1}, two modes with large wag(NH_2) PED contribution are assigned to the intense bands observed at 470 cm^{-1} and 460 cm^{-1}, respectively. Detailed comparison of the experimentally observed and theoretically predicted frequencies in Table 2 leads to a mean frequency deviation $\overline{\Delta\nu} = \left|\overline{\nu_{exp} - \nu_{th}}\right| = 16$ cm^{-1} (RHF) or 12 cm^{-1} (DFT) for 4–NH_2–benzimidazole. This demonstrates that the applied DFT (B3LYP)/6–31++G** theoretical methodology is sufficiently accurate to perform reliable assignments.

Table 3. Experimental (Ar matrix) and calculated (RHF and DFT–B3LYP)/6–31++G**) vibrational data for 7–NH_2–benzimidazole

Experimental ν (cm^{-1})	Calculated ν (cm^{-1})			Experimental [a] I (km mol^{-1})		Calculated A (km mol^{-1})		PED [e]		
	RHF [b]	DFT [c]	DFT [d]	RHF	DFT	RHF	DFT	Mode	RHF	DFT
3528/3525	3532	3560	3486	65	34	109	63	$\nu(N_1H)$	100	100
3495?	3474	3522	3450	[g]		15	11	$\nu^a(NH_2)$	95	97
3362	3380	3424	3353	7	4	9	3	$\nu^s(NH_2)$	95	97
3076?	3077	3156	3090	[g]		5	2	$\nu(C_2H)$	99	99
3066?	3045	3122	3058	[g]		10	8	$\nu(C_4H)$	87	76
3043?	3022	3097	3033	[g]		18	15	$\nu(C_5H)$	68	77
								$\nu(C_6H)$	19	14
3026?	3002	3076	3012	[g]		13	14	$\nu(C_6H)$	80	85
								$\nu(C_5H)$	19	14
1635	1640	1624	1633	[g]		6	4	$\delta(NH_2)$	15	24
								$\nu(C_7C_8)$	18	19
1631?	1629	1616	1624	[g]		117	120	$\delta(NH_2)$	44	50
1606	1599	1586	1594	10	5	13	20	$\nu(C_4C_9)$	–	19
								$\delta(NH_2)$	24	–
1559	1532	1497	1504	38	20	65	3	$\nu(C_2N_3)$	59	36
								$\delta(C_2H)$	19	11
1475	1501	1491	1499	9	5	18	48	$\nu(C_2N_3)$	–	23
								$\delta(C_5H)$	29	17
								$\nu(C_4C_5)$	15	–
1458?	1432	1420	1427	[g]		23	13	$\delta(C_4H)$	25	25
								$\nu(C_8C_9)$	22	18
1358	1406	1389	1397	139	72	139	72	$\delta(N_1H)$	47	35
								$\nu(N_1C_2)$	22	12
1333?	1284	1351	1358	[g]		25	34	$\nu(C_8C_9)$	–	14
								$\nu(N_1C_2)$	16	11
								$\nu(C_7N)$	18	–
								$\rho(NH_2)$	16	–
1296/1291/1286	1329	1305	1312	13	7	22	8	$\delta(C_2H)$	31	24
								$\nu(C_2N_3)$	19	22
[f]	1242	1281	1287			43	56	$\delta(C_6H)$	24	25
								$\nu(C_7N)$	–	24
								$\nu(N_3C_9)$	–	15
								$\delta(C_4H)$	18	–
1257?	1256	1246	1253	[g]		15	24	$\delta(C_4H)$	–	17
								$\delta(C_5H)$	24	16
								$\nu(N_3C_9)$	25	14
[h]	1198	1197	1203			3	0.7	$\delta(C_2H)$	23	26
								$\delta(R1)$	21	16
								$\nu(N_1C_8)$	20	14
[h]	1142	1150	1156			2	0.3	$\delta(C_5H)$	18	25
								$\delta(C_4H)$	15	23
								$\rho(NH_2)$	21	–
[h]	1102	1115	1121			2	6	$\rho(NH_2)$	21	41
								$\delta(C_6H)$	15	18
1083?	1073	1069	1075	[g]		23	10	$\nu(N_1C_2)$	61	55
								$\delta(N_1H)$	23	22
1057/1052?	1034	1040	1046	[g]		12	16	$\nu(C_4C_5)$	21	22
								$\nu(C_5C_6)$	24	19
								$\delta(C_4H)$	14	15

Table 3. (Continued)

Experimental ν (cm^{-1})	Calculated ν (cm^{-1})			Experimental [a] I (km mol^{-1})		Calculated A (km mol^{-1})		PED [e]		
	RHF [b]	DFT [c]	DFT [d]	RHF	DFT	RHF	DFT	Mode	RHF	DFT
1009?	1008	1002	1007	[g]		20	15	$\rho(NH_2)$	11	19
								$\nu(C_5C_6)$	16	13
[h]	982	933	943			1	0.6	$\gamma(C_5H)$	67	60
								$\gamma(C_4H)$	33	30
[h]	922	917	922			2	0.1	δ(r1)	29	41
								δ(r2)	25	33
								$\nu(C_8C_9)$	13	16
								$\gamma(C_2H)$	26	–
908?	894	851	860	[g]		7	2	$\gamma(C_6H)$	60	55
								$\gamma(C_4H)$	35	37
842	837	837	842	39	20	39	10	δ(R1)	37	42
913?	918	829	837	[g]		7	19	$\gamma(C_2H)$	76	95
941	804	776	784	92		137	72	τ(R1)	–	16
								$\gamma(C_6H)$	–	15
								$wag(NH_2)$	18	–
742	733	720	728	[g]		26	65	τ(R1)	38	32
								$\gamma(C_5H)$	15	17
								$\gamma(C_4H)$	11	15
954	758	706	713	56	29	91	144	$Wag(NH_2)$	42	57
								$\gamma(C_6H)$	15	13
[h]	663	672	676			4	12	$\nu(C_4C_9)$	23	19
[h]	645	639	645			8	13	τ(r1)	55	55
								τ(r2)	20	23
[h]	591	592	595			3	2	δ(r2)	26	27
								$\nu(C_7C_8)$	21	20
								δ(R3)	16	17
557	572	568	574	3	2	8	14	τ(r2)	40	38
								τ(R3)	32	29
								τ(R1)	25	23
530	532	532	537	4	2	6	9	τ(R2)	32	30
								$\gamma(C_7N)$	29	27
								τ(R1)	15	18
[h]	493	493	495			2	1	δ(R2)	52	59
473	470	472	475	[e]		5	6	δ(R3)	22	26
								$\delta(C_7N)$	19	21
								δ(R2)	18	12
457	418	412	417	118	61	155	110	$\gamma(N_1H)$	96	96
[i]	282	281	284			12	14	τ(R3)	42	39
								τ(R2)	18	15
								τ(r2)	15	12
[i]	259	264	265			4	2	$\delta(C_7N)$	47	37
								δ(R3)	18	15
[i]	154	235	238			40	20	$\tau(NH_2)$	94	51
								τ(Rr)	–	20
[i]	214	196	198			10	19	τ(Rr)	67	49
								$\tau(NH_2)$	–	31
								τ(R2)	15	–
[i]	183	178	180			3	3	τ(R2)	43	49
								$\gamma(C_7N)$	–	17
								τ(R1)	15	15

Table 3. (Continued)

[a] Experimental intensity normalized to the calculated value of $\delta(N_1H)$ at 1406 cm^{-1} (139 $km.mol^{-1}$) at the RHF and 1389 cm^{-1} (72 $km.mol^{-1}$) at the DFT level of theory

[b] Uniform scaling factor 0.900

[c] Uniform scaling factor 0.970

[d] Variable scaling factor applied

[e] Only contributions ≥ 15 % are reported; ν designates stretching, δ bending, τ torsion, wag wagging, γ out–of–plane vibration, and ρ rocking mode; NH_2 modes are further indicated with "s" for symmetric and "a" for asymmetric; R and r refer to the six and five ring part, respectively

[f] Overlap with a band of 4–NH_2–benzimidazole

[g] Not measurable due to neighboring 4–NH_2–benzimidazole absorption

[h] Too weak to be observed

[i] Situated below the studied region (< 400 cm^{-1})

For the rare tautomer 7–NH_2–benzimidazole a limited number of assignments are given in Table 3. It appears that the assignments for 7–NH_2–benzimidazole can only be partly performed due to overlap or proximity with absorptions of 4–NH_2–benzimidazole or to a weak intrinsic intensity combined to the small abundance of this tautomer. However, most of the NH_2 and N–H modes can be assigned. This allows to conclude that the NH_2 stretching vibrations have smaller frequencies in the 7–NH_2–benzimidazole form, while $\delta(NH_2)$ and $\rho(NH_2)$ are comparable for both tautomers. A particularly large deviation is observed between the wag(NH_2) modes, *i.e*. 460 cm^{-1} for the 4–NH_2– and 954 cm^{-1} for the 7–NH_2–benzimidazole (see further). The N_1–H group has slightly larger stretching, bending and out–of–plane frequencies in the 4–NH_2 form. Taking into account the inaccuracy of some of the assignments for 7–NH_2–benzimidazole, the mean frequency deviation $\overline{\Delta\nu} = \left|\overline{\nu_{exp} - \nu_{th}}\right| = 14$ or 11 cm^{-1}, at the RHF and DFT level, respectively.

3.3 Tautomerization Constant K_T

An experimental estimation of a tautomerization constant K_T value for a tautomeric coexistence in the gas phase or a low–temperature matrix can be obtained by application of the Lambert–Beer law for IR absorption, $I_i = \varepsilon_i c_i d$, with c_i the concentration of absorbing species, d the path length of the sample measured and ε_i the extinction coefficient. Application of this relation to two coexisting tautomers 1 and 2 in the same matrix leads to [24,25]:

$$K_T = \frac{c_1}{c_2} = \left(\frac{I_1}{I_2}\right)\left(\frac{\varepsilon_2}{\varepsilon_1}\right) \qquad (1)$$

The values of ε_1 and ε_2 are not known. Two acceptable approximations have been proposed. One can use the theoretically calculated 'intrinsic' intensity A_i for ε_i, or one can use the ratio of the total intensities $\sum_1 A_1 \Big/ \sum_2 A_2$ predicted for all the vibrational modes. The latter method is used by the Warsow–group of M. Nowak, whereas we prefer to use the first and simpler method. As a matter of fact, both methods yield only slightly different K_T values, in view of the estimation limit, *i.e*. 0.40

and 0.33 for 2–OH–pyridine [26]. The former description allows us to use the following formula for estimation of the experimental K_T value:

$$K_T(7AB/4AB) = \frac{I(\nu_{7AB})/A(\nu_{7AB})}{I(\nu_{4AB})/A(\nu_{4AB})} \quad (2)$$

with $I(\nu_i)$ the experimental intensity and $A(\nu_i)$ the theoretically predicted intensity.

At last, many former results obtained by our research group have demonstrated that K_T values obtained by matrix–isolation IR spectroscopy reflect well the tautomeric gas phase equilibrium, *e.g.* 2–OH–pyridine K_T(Ar) = 2.2 [23,26] versus K_T(gas) = 2.5 [27].

Table 4. Experimental estimation of the tautomerization constant K_T(7ABIM/4ABIM) for 4(7)–NH_2–benzimidazole at the DFT (B3LYP) / 6–31++G** level

Frequency 4ABIM	Frequency 7ABIM							
	3362	1606	1296	954	941	557	530	457
3517	0.22	0.33	0.17	0.27	0.11	0.19	0.30	0.26
3506	0.21	0.16	0.06	0.13	0.43	0.09	0.15	0.35
3423	0.29	0.22	0.12	0.18	0.29	0.26	0.20	0.49
1516	0.42	0.42	0.24	0.46	0.48	0.33	0.49	0.27
1493	0.47	0.09	0.30	0.27	0.23	0.05	0.09	0.19
1443	0.30	0.13	0.46	0.11	0.35	0.07	0.12	0.29
1393	0.21	0.12	0.33	0.30	0.33	0.50	0.22	0.51
1335	0.21	0.23	0.20	0.20	0.44	0.13	0.20	0.50
1229	0.44	0.43	0.67	0.35	0.14	0.24	0.38	0.05
1189	0.33	0.25	0.13	0.20	0.33	0.29	0.22	0.55
1080	0.24	0.18	0.09	0.14	0.21	0.21	0.16	0.40
1065	0.28	0.67	0.43	0.53	0.56	0.38	0.59	0.31
1015	0.28	0.21	0.11	0.17	0.28	0.24	0.18	0.33
852	0.27	0.21	0.11	0.17	0.27	0.24	0.18	0.46
834	0.33	0.25	0.13	0.20	0.67	0.29	0.22	0.55
730	0.22	0.17	0.34	0.67	0.45	0.48	0.26	0.54
470	0.28	0.21	0.11	0.17	0.28	0.25	0.19	0.47
460	0.33	0.25	0.13	0.20	0.33	0.29	0.22	0.56
Average K_T								0.28 ± 0.14 [a]

[a] $\sum_n \frac{x_i}{n} \pm \sqrt{\frac{n\sum x^2 - (\sum x)^2}{n(n-1)}}$

Not all the assigned bands of the 4–NH_2– and 7–NH_2–benzimidazole (Tables 2 and 3) could be used because of doubtful experimental intensity values. One possible reason for such a doubtful experimental intensity is overlap or closeness of bands, which yields too large experimental intensities compared to the theoretical ones. This, for instance, is the case for the band of 1253 cm^{-1} for 4–NH_2–benzimidazole which overlaps with the band at 1257 cm^{-1} for the 7–NH_2 form. The same holds for the doublet located at 1623/1631 cm^{-1} for the 4–NH_2 tautomer, which has a too large experimental intensity due to overlap with the doublet of 7–NH_2–benzimidazole at 1635/1631 cm^{-1}. Table 4 lists the obtained K_T values for 144 different combinations of band pairs. Mean K_T values

of 0.28 or 0.31 are obtained, depending on whether DFT (Table 4) or RHF predicted intensities are used.

The problem for obtaining the 'theoretical' K_T–value is somewhat more complicated. The exact formula to be used for the theoretical K_T value is

$$\Delta G_T^\circ = -RT \ln K_T \tag{3}$$

with ΔG_T° the free enthalpy difference at temperature T for the tautomeric interconversion.

One usually assumes that ΔG° (at temperature T) = ΔH° – TΔS° (at temperature T) can be replaced by ΔE° at 0 K. This approximations involves two –at first sight– drastic approximations, i.e. neglectance of the temperature dependence of ΔH° from 0 K to working temperature as well as of the term TΔS°. Both assumptions have been demonstrated to be acceptable for tautomeric equilibria by Kwiatkowski *et al*. [28]. The calculations performed in this work once again demonstrate this : ΔS° is for both tautomers as small as 2.33 J/K.mole at 0 K and about 0.8 kJ/mole at 340 K, whereas ΔE° ≅ 13 kJ/mole (see further). It means that, even over a temperature range as large as 340 K, the term TΔS° only contributes for less than 10 %. On the other hand, if we use the ΔG° values at 340 K (15.49 kJ/mole) from the Gaussian outputs, we obtain K_T = 0.004 instead of K_T = 0.003 for ΔE° (0 K). This allows us to use ΔE° (0 K) instead of ΔG°(T) for a theoretical estimation of the order of magnitude of K_T.

Using the above equation with ΔE_T values obtained by the RHF and DFT (B3LYP) calculations, a theoretical K_T value of 0.007 (RHF) or 0.003 (DFT) is obtained, respectively. This is considerably smaller than the experimental K_T value. Nowadays it is generally accepted that tautomerization is not unimolecular, but proceeds by an H–bonded assisted mechanism in which short living dimers [29] or water complexes [30] play an important role. For instance, the water–assisted proton transfer has been shown to increase the population of the rare tautomer by lowering the activation energy barrier for the intramolecular proton transfer [30,31]. In one of our earlier studies for 2–OH–pyridine ⇆ 2–pyridone it has been demonstrated that the matrix tautomeric equilibrium shifts towards the rare oxo form by the presence of water [23].

3.4 Non–planarity of the NH_2 Group

The most important observation in the vibrational analysis is the location of the wag(NH_2) mode. As a matter of fact, a substantial discrepancy is noticed between the calculated and experimental values of the wag(NH_2) frequency and intensity. This discrepancy is found between the experimental frequencies (470/460 cm^{-1} for 4AB *vs*. 954/941 cm^{-1} for 7AB) as well as between the deviation of experimental and theoretical frequencies (*e.g*. 470 ↔ 518 cm^{-1} for 4AB *vs*. 954 ↔ 713 cm^{-1} for 7AB). The latter effect is striking, since observation of a substantially larger experimental frequency than theoretically predicted is extremely unusual. We have investigated whether this observation is due to a larger degree of non–planarity of the NH_2 group with the aromatic six ring.

It is well known that the C–NH_2 bond in cytosine (1.364 Å) and purines is considerably shorter than a pure, single C–N bond (1.472 Å) and that it has ± 45% double bond character, which indicates a large degree of co–planarity of the NH_2 group with the six ring [15].

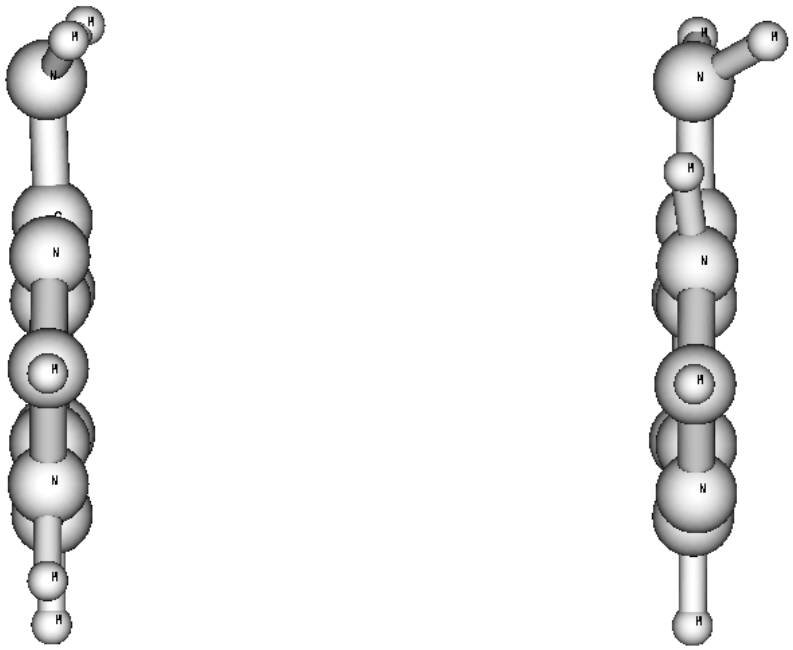

Figure 4. Side projection of 4–NH_2–benzimidazole (left) and 7–NH_2–benzimidazole (right).

In order to obtain detailed information on the co–planarity of the NH_2 group, we have compared some important geometry parameters of the amino groups in 4–NH_2– and 7–NH_2–benzimidazole, as well as in 2–NH_2–purine [32] and 6–thioguanine [33]. Two relevant parameters are: the distance between the amino N and the vicinal C atom in the six ring and the three angles $\hat{HNC}$, $\hat{HNH}$ and $\hat{HNC}$ around the amino N atom. A further interesting parameter is the sum of these three angles, since this sum is 360° only in case of perfect co–planarity of the NH_2 group with the six–membered ring, which is clearly not the case here (Figure 4). In addition, the Cartesian Z–coordinates of the three atoms of the amino group are listed in Table 5.

In first instance, the degree of co–planarity is evaluated from the sum of the 3 angles around the amino N–atom. Table 5 demonstrates that for 7–NH_2–benzimidazole a larger deviation from co–planarity is observed than for 4–NH_2–benzimidazole. The larger Z–coordinate for the H–atom adjacent to the N–H group gives also evidence for a larger deviation of co–planarity. This is illustrated in Figure 4 where a side view of the non–planar 7–amino tautomer is shown in comparison with the more planar 4–amino tautomer. All these observations suggest a substantial repulsion between the amino N–H bond adjacent to the NH bond at N_1 in 7–NH_2–benzimidazole. The role of the adjacent N–H bond close to the amino group is further demonstrated by the comparable results for the amino–N_3H and amino–N_1H tautomers of 2–NH_2–purine and for the amino–thione–N_1H–N_7H and amino–thione–N_1H–N_9H tautomers of 6–thioguanine (Table 5). These

structural deviations between 4–NH_2–benzimidazole and its 7–NH_2 tautomer are also manifested by the frequency values of the amino modes. The in–plane δ and ρ modes are not used in this analysis because these modes are strongly coupled with other modes while for the torsion modes only theoretical data are available. The ν^a and ν^s modes are different, but these differences are rather limited.

Table 5. Geometrical parameters for 4(7)–aminobenzimidazole, four amino tautomers of 2–aminopurine and three tautomers of 6–thioguanine, calculated at the RHF and DFT(B3–LYP) level of theory (6–31++G** basis set)

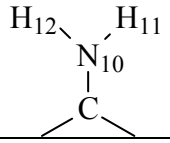

Molecule		Angles (°)				Distance (Å)	Cartesian Z–coordinate		
		$CN_{10}H_{11}$	$CN_{10}H_{12}$	$H_{11}N_{10}H_{12}$	sum	CN_{10}	N_{10}	H_{11}	H_{12}
4(7)–aminobenzimidazole									
4–Amino	RHF	114.86	116.06	113.57	344.49	1.382	-0.6956	0.1773	0.3194
	DFT	115.31	117.08	114.45	346.84	1.386	-0.0700	0.1584	0.2904
7–Amino	RHF	112.66	112.63	109.01	**334.30**	1.412	0.0190	**0.7730**	-0.1805
	DFT	113.87	113.04	109.46	**336.37**	1.412	-0.0547	**0.6517**	-0.0179
2–aminopurine									
Amino–N9H	RHF	116.98	117.40	118.10	352.48	1.358	-0.0500	0.1667	0.1725
	DFT	117.04	117.64	118.36	353.04	1.369	-0.0516	0.1593	0.1626
Amino–N7H	RHF	116.64	116.44	117.43	350.51	1.363	-0.0565	0.1979	0.1827
	DFT	117.05	116.84	118.03	351.92	1.372	-0.0570	0.1796	0.1634
Amino–N3H	RHF	117.42	112.58	113.69	**343.69**	1.370	-0.0608	**0.4497**	0.0555
Amino–N1H	RHF	113.77	118.47	114.97	**347.21**	1.363	-0.0560	0.0881	**0.3655**
6–thioguanine									
Amino–thiol–N9H – rot 1	RHF	117.46	117.70	118.58	353.74	1.355	-0.0449	0.1520	0.1597
	MP2	114.68	114.96	115.63	345.27	1.379	-0.0897	0.2116	0.2123
	DFT	117.32	117.64	118.55	353.51	1.368	-0.0485	0.1538	0.1608
Amino–thione–N1H–N7H	RHF	118.47	113.72	114.89	347.08	1.363	-0.0559	0.3683	0.0881
	MP2	115.37	110.78	111.90	**338.05**	1.389	-0.0829	**0.5319**	0.0089
	DFT	118.35	113.04	114.42	345.81	1.377	-0.0611	0.3930	0.0832
Amino–thione–N1H–N9H	RHF	119.30	114.92	115.88	350.10	1.357	-0.0506	0.2972	0.1042
	MP2	115.94	111.74	112.61	**340.29**	1.385	-0.0795	**0.4662**	0.0609
	DFT	118.83	114.07	115.10	348	1.373	-0.0581	0.3356	0.1040

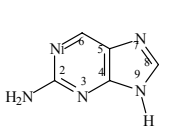
amino–N_9H

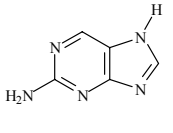
amino–N_7H

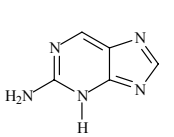
amino–N_3H

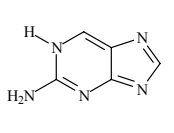
amino–N_1H

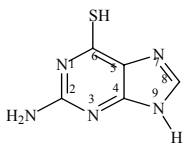
amino–thiol–N_9H

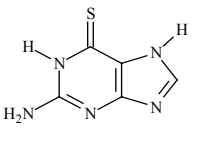
amino–thione–N_1H–N_7H

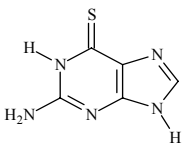
amino–thione–N_1H–N_9H

On the other hand, the mode with largest wag(NH_2) contribution for 7–NH_2–benzimidazole is predicted at 758 cm^{-1} and 713 cm^{-1} at the RHF and DFT level, respectively, while this mode is assigned to the band at 954 cm^{-1} in the experimental spectrum. This implies a frequency deviation as large as 240 cm^{-1} (DFT). The "optimal" scaling factor (ν_{exp}/ν_{theor}) for the two modes with large wag(NH_2) contribution in 7–NH_2–benzimidazole is 1.17 and 1.20 (RHF) or 1.20 and 1.34 (DFT), whereas for 4–NH_2–benzimidazole (460 and 470 cm^{-1}) it is 0.77/0.79 (RHF), or 0.89/0.91 (DFT). Taking into account the last values, the difference with the "uniform" scaling factors (0.900 for RHF, 0.970 for DFT) indicates a strong anharmonicity of the wag(NH_2) mode in 4–NH_2–benzimidazole. Also for 4–NH_2–pyridine an optimal scaling factor of 0.84 was obtained at the RHF level of theory [34]. However, the most striking observation is the optimal scaling factor much larger than 1.0 for the wag(NH_2) modes in 7–NH_2–benzimidazole. This would indicate a kind of "reversed" anharmonicity, *i.e.* a vibrational mode with less than 'zero anharmonicity'.

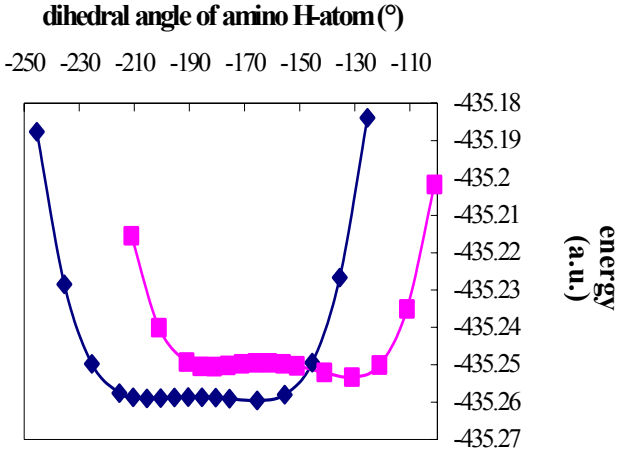

Figure 5. Potential energy curves for the wag(NH_2) mode in 4–NH_2–benzimidazole (◆)and 7–NH_2–benzimidazole (■).

Table 6. Calculated (DFT–B3LYP/6–31++G**) energy values (a.u), change of dihedral angle (°) and energy differences ΔE_T (kJ mol^{-1}) during the NH_2 wag motion for 4–NH_2–benzimidazole and 7–NH_2–benzimidazole.

Calculated Energy (a.u.)	Change of dihedral angle (°)	Calculated Energy (a.u.)	Change of dihedral angle (°)
4–NH_2–benzimidazole		7–NH_2–benzimidazole	
–435.183928	–40	–435.201744	–30
–435.226680	–30	–435.235080	–20
–435.249451	–20	–435.250072	–10
–435.258027	–10	–435.253330	0
–435.259577	0	–435.252045	10
–435.259115	10	–435.250318	20
–435.258847	15	–435.249763	25
–435.258694	20	–435.249488	30
–435.258678	25	–435.249499	35
–435.258786	30	–435.249762	40
–435.258952	35	–435.250178	45
–435.259027	40	–435.250538	50
–435.258731	45	–435.250446	55
–435.257597	50	–435.249282	60
–435.249800	60	–435.240107	70
–435.228490	70	–435.215503	80
–435.187672	80		

The explanation of this phenomenon is based on the consideration that for 7–NH_2–benzimidazole, the wag(NH_2) mode implies a movement near the neighboring, disturbing N–H group, which results in a higher energy (repulsion) and therefore a higher frequency compared to the same mode in 4–NH_2–benzimidazole. This hindrance can explain why for 7–NH_2–benzimidazole even an experimental frequency higher than the unscaled theoretical (842 cm^{-1} (RHF) and 735 cm^{-1} (DFT)) value is observed. A theoretical simulation of this out–of–plane motion of the non–planar amino group was performed for both tautomers. For this purpose, the two dihedral angles of the amino hydrogens were varied while optimizing the remaining geometrical parameters. The results of these calculations are shown in Table 6 and Figure 5.

This Figure demonstrates that the amino wag mode is, for both tautomers, described by a double minimum potential along the internal coordinate, as can be expected from the existence of two stable conformational structures with the exocyclic amino group at either side of the aromatic plane. Moreover, the fact that the hydrogens of the amino group are characterized by non–symmetrical dihedral angles with respect to the aromatic plane (–26/+26 and –165/+165 for both conformations of the 4–amino and –5/+5 and –131/–131 for the 7–amino form) implies that the wag motion of one conformation never can result in an equally stable, mirror conformation during the described motion from one side of the plane to the other. Also, the larger energy barrier for the 7–NH_2 tautomer (10 kJ mol^{-1} versus 2 kJ mol^{-1}) reflects the larger steric hindrance exerted by the adjacent N–H group of the imidazole ring during the wag motion of the NH_2 group. The most important observation, however, is that the slope of the potential from the minimum (dihedral angle –131° for 7–NH_2 and –165° for 4–NH_2 in Figure 5, where only one of the two dihedral angles is plotted) towards larger negative dihedral angles is considerably larger for 7–NH_2–benzimidazole than for 4–NH_2–benzimidazole. As a matter of fact, the potential increase for a 25° negative increase of the dihedral angle is 4.4×10^{-5} a.u./° for the 4–NH_2 form, whereas it is 15×10^{-5} a.u./° for the 7–NH_2 form (Table 5). The much steeper potential curve in this region around the equilibrium dihedral angle reflects a decreased anharmonicity, which is consistent with the observed larger wag(NH_2) frequency.

4 CONCLUSIONS

The matrix–isolation FT–IR method combined with DFT (B3LYP) and RHF calculations using a 6–31++G** basis set has been used for the study of the intrinsic tautomeric properties of 4(7)–NH_2–benzimidazole. In addition to a rather complete IR–analysis with nearly all the observed bands assigned to the presence of both tautomers, this study yields an average experimental K_T(7–NH_2–benzimidazole/4–NH_2–benzimidazole) value of 0.28 (DFT). On the other hand, theoretical estimations of the tautomerization constant are 0.003 (DFT) and 0.007 (RHF). This implies that the rare 7–amino tautomer is present for about 22% in an inert Ar matrix. The large discrepancy

between theoretically predicted and experimental values for the wag(NH_2) mode of the 7–NH_2 form is explained by the presence of a smaller anharmonicity which has been supported by a potential calculation for this vibrational mode in the two tautomeric forms. This calculation has resulted in an asymmetric double minimum potential for both tautomers, but with increased asymmetry and smaller anharmonicity in case of the 7–amino tautomer. This demonstrates the large steric hindrance by passing the adjacent N–H group of the imidazole ring during the wag motion, a phenomenon which is also observed in other compounds with NH groups adjacent to an excocyclic NH_2 group. This work also demonstrates again that the applied DFT (B3–LYP)/6–31++G** theoretical methodology is excellent for both tautomeric and vibrational prediction of large polyfunctional molecules such as the studied compound 4(7)–aminobenzimidazole.

Acknowledgment

L. Houben acknowledges the K.U. Leuven for a FLOF grant during her Ph.D. studies. Riet Ramaekers thanks the Flemish Fund for Scientific Research (F.W.O.–Vlaanderen) for the postdoctoral fellowship.

5 REFERENCES

[1] M. Graindourze, J. Smets, Th. Zeegers–Huyskens and G. Maes, *J. Mol. Struct.* **1990**, *222*, 345.
[2] M. Graindourze, T. Grootaers, J. Smets, Th. Zeegers–Huyskens and G. Maes, *J. Mol. Struct.* **1991**, *243*, 37.
[3] G. Maes and J. Smets, *J. Phys. Chem.* **1993**, *97*, 1818.
[4] J. Smets, L. Adamowicz and G. Maes, *J. Mol. Struct.* **1994**, *322*, 113.
[5] G. Maes, J. Smets and L. Adamowicz, in *Low Temperature Molecular Spectroscopy*, NATO ASI Series, R. Fausto (Ed.), Kluwer Acad. Publ., 1996, pp. 147–167.
[6] M. K. Van Bael, K. Schoone, L. Houben, J. Smets, W. McCarthy, L. Adamowicz, M. J. Nowak and G. Maes, *J. Phys. Chem.* **1997**, *101*, 2397.
[7] K. Schoone, J. Smets, L. Houben, M. K. Van Bael, L. Adamowicz and G. Maes, *J. Phys. Chem. A* **1998**, *102*, 4863.
[8] K. Schoone, G. Maes and L. Adamowicz, *J. Mol. Struct.* **1999**, *480–481*, 505.
[9] A. Dkhissi, L. Houben, J. Smets, L. Adamowicz and G. Maes, *J. Phys. Chem. A*, **2000**, *104*, 43, 9785.
[10] R. Ramaekers, A. Dkhissi, L. Adamowicz and G. Maes, *J. Phys. Chem. A* **2002**, 106, 4502.
[11] L. Houben, *Ph.D. Thesis*, KULeuven, 2000.
[12] E. C. Fisher and M. M. Joullié, *J.Org.Chem.* **1958**, *23*, 1944.
[13] G. M. Van Der Want, *Rec.Trav.Chem.* **1948**, *67*, 45.
[14] A. Marcos, C. Pedregal and C. Avendano, *Tetrahedron* **1991**, *47*, 35, 7459.
[15] W. Saenger in Springer Advanced Texts in Chemistry: Principles of Nucleic Acid Chemistry, Cantor, C.R. (Ed.), Springer–Verlag: New York, 1984.
[16] A. D. Becke, *J. Chem. Phys.* **1993**, *98*, 5648.
[17] C. Lee, W. Yang and R.G. Parr, *Phys. Rev.* **1988**, *B37*, 785.
[18] M.J. Frisch, G. W. Trucks, H. B. Schlegel, P. M. W. Gill, B. G. Johnson, M. A. Robb, J. R. Cheeseman, T. Keith, G. A. Petersson, J. A. Montgomery, K. Raghavachari, M. A. Al–Laham, V. G. Zakrzewski, J. V. Ortiz, J. B. Foresman, C. Y. Peng, P. Y. Ayala, W. Chen, M. W. Wong, J. L. Andres, E. S. Replogle, R. Gomperts, R. L. Martin, D. J. Fox, J. S. Binkley, D. J. Defrees, J. Baker, J. P. Stewart, M. Head–Gordon, C. Gonzalez and J. A. Pople, J.A. *Gaussian94*; Revision C.3.; Gaussian Inc.: Pittsburgh, PA, 1995.
[19] J. Florian and B. G. Johnson, *J. Phys. Chem.* **1994**, *98*, 3681.
[20] G. Rauhut and P. Paulay, *J. Phys. Chem.* **1995**, *99*, 3093.
[21] J. Florian and J. Leszczynski, *J. Phys. Chem.* **1996**, *100*, 5578.
[22] G. Maes, *Bull. Soc. Chim. Belg.* **1981**, *90*, 1093.
[23] A. Dkhissi, L. Houben, J. Smets, L. Adamowicz and G. Maes, *J. Mol. Struct.* **1999**, *484*, 215.
[24] M. J. Nowak, K. Szczepaniak, A. Baustin and D. Shugar, *J. Mol. Struct.* **1980**, *62*, 47.
[25] D. Shugar and K. Szczepaniak, *J. Quant. Chem.* **1981**, *20*, 573.

[26] J. Smets and G. Maes, *Chem*. *Phys*. *Lett*. **1991**, *187*, 532.
[27] C. Guimon, G. Garrabe and G. Pfister–Guillozo, *Tetrahedron Lett*. **1979**, 2585.
[28] J. S. Kwiatkowski and J. Leszczynski, *Chem*. *Phys*. *Lett*. **1993**, *204*, 430.
[29] M. J. Field and I. H. Hillier, *J*. *Chem*. *Soc*. *Perkin Trans*. *II* **1987**, *2*, 617.
[30] W. M. F. Fabian, *J*. *Phys*. *Org*. *Chem*. **1990**, *3*, 332.
[31] J. Gu and J. Leszczynski, *J*. *Chem*. *Phys*. *A* **1999**, *103*, 2744.
[32] R. Ramaekers, L. Adamowicz and G. Maes, *Europ*. *Phys*. *J*. *D*. **2002**, *20*, 375.
[33] R. Ramaekers, PhD Thesis, University of Leuven (2001).
[34] J. Smets, L. Adamowicz and G. Maes, *J*. *Phys*. *Chem*. **1995**, *99*, 6387.